Synthesis, X-ray Crystal Structure, and Chemistry of a Metal Cluster Ketenylidene, $[Fe_3(CO)_9(CCO)]^{2-}$, with Carbide-like Reactivity

Joseph W. Kolis,[1a,b] Elizabeth M. Holt,*[1c] and Duward F. Shriver*[1a]

Contribution from the Departments of Chemistry, Northwestern University, Evanston, Illinois 60201, and Oklahoma State University, Stillwater, Oklahoma 74078.
Received June 9, 1983

Abstract: The acylation of a bridging CO in $[Fe_3(CO)_{11}]^{2-}$ followed by reductive cleavage produces a compound that has the chemical properties of an exposed carbide but possesses the structure of a ketenylidene. This compound reacts with H^+ and CH_3^+ sources to produce a cluster-bound methyne or ethyne, respectively. In both cases the CO that formerly was part of the ketenylidene has migrated onto the metal cluster. The X-ray crystal structures of the methyne, $[Fe_3(CO)_{10}(CH)]^{2-}$, and ketenylidene, $[Fe_3(CO)_9(CCO)]^{2-}$, were determined, and the CCO ligand in the latter cluster was found to be tipped by 33° relative to a plane vertical to the Fe_3 plane. This structural feature may be related to the facile reaction of the CCO ligand with electrophiles.

Metal cluster carbides that are reactive at the carbide have been discovered only recently.[2] This class of compounds opens the possibility of new synthetic organometallic chemistry based on the carbide ligand, and it also provides the opportunity for developing molecular chemistry analogous to Fischer–Tropsch chemistry in which a surface carbide is implicated.[3] The known reactive carbides are isoelectronic four-iron species, Ia and Ib,

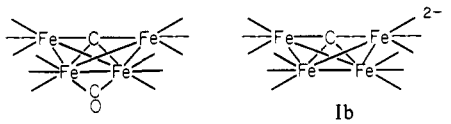

Ia Ib

in which the low coordination of the carbide appears to be responsible for its reactivity.[2,4-6] Conventional synthetic routes to carbides, which generally employ elevated temperatures, yield the less reactive enclosed carbide cluster compounds. The importance of exposed carbide clusters prompted the development of a new method for the synthesis of carbides under mild conditions.[7,8] The basis of this synthesis is the alkylation or acylation of a carbonyl oxygen followed by reductive cleavage of the activated CO (eq 1).

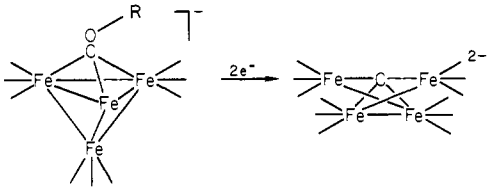

(1)

In an earlier communication we reported the application of this synthetic procedure to a three-iron system, with the thought that the greater exposure of the carbide ligand in the lower nuclearity cluster would lead to high reactivity at the carbide.[8] On the basis of spectroscopic evidence, the product of that reaction was described as $[Fe_3(CO)_9(CCO)]^{2-}$ rather than a carbide, even though the reactions mimic those of an exposed carbide. The present paper describes this chemistry and the characterization of this product in greater detail. Also, several bonding models are discussed in connection with the unusual structure and reactivity of $[Fe_3(CO)_9(CCO)]^{2-}$.

Experimental Section

General Procedures. All reactions were carried out under a purified nitrogen atmosphere by standard syringe and Schlenk techniques.[9] Tetrahydrofuran and CH_2Cl_2 were rigorously dried and degassed before use. Anhydrous diethyl ether (Mallinckrodt) and reagent grade methanol (Mallinckrodt) were bubbled with N_2 before use. Acetyl chloride was purified by distillation from PCl_5 followed by vacuum distillation from quinoline; CH_3I, CF_3COOH, and CF_3SO_3H were distilled before use. Bis(triphenylphosphine)nitrogen(1+) chloride ([PPN]Cl) (Alfa-Ventron), tetraphenylarsonium chloride ($[Ph_4As]Cl$) (Alfa-Ventron), $Fe_3(CO)_{12}$ (Strem), and 40% Na/mineral oil (Aldrich) were used as received. $[PPN]_2[Fe_3(CO)_{11}]$ was prepared by a literature method,[10] and an analogous procedure was followed for $[Ph_4As]_2[Fe_3(CO)_{11}]$. Infrared spectra were obtained on a Perkin-Elmer 339 spectrometer. ^1H and ^{13}C NMR were obtained on a JEOL FX-270 spectrometer. Elemental analyses were performed by Galbraith Laboratories.

Synthesis of $[PPN]_2[Fe_3(CO)_9(CCO)]$ (II). A 2.5-g sample of $[PPN]_2[Fe_3(CO)_{11}]$ was dissolved in 15 mL of CH_2Cl_2, and 1.0 mL of acetyl chloride was added with stirring. After 20 min, the orange solution had turned red-brown and 60 mL of Et_2O was added. The white [PPN]Cl was filtered off and the solvent removed from the filtrate under vacuum. In the meantime, a reducing solution consisting of 0.5 g of Na dispersion and 2 g of benzophenone in 60 mL of THF was stirred for $^1/_2$ h. The acetyl cluster, $[PPN][Fe_3(CO)_{10}(COCOCH_3)]$, was dissolved in 5 mL of THF, and the reducing solution added dropwise with stirring. The reaction was monitored by IR, and addition of the reducing solution was stopped when bands at 1992 and 1970 cm^{-1} disappeared (bands at 1925 and 1870 cm^{-1} grew in during the reaction). The reaction mixture was filtered and the THF removed under vacuum. The orange oil was redissolved in 15 mL of CH_2Cl_2, 1.2 g of fresh [PPN]Cl added, the solution filtered, and the filtrate layered with 50 mL of Et_2O.

After standing for 24 h, a crop of large red-orange needles was collected by filtration and washed several times with MeOH and Et_2O; yield 1.7 g (68%). Anal. Calcd for $C_{83}H_{60}N_2O_{10}P_4Fe_3$: C, 64.87; H, 3.94; N, 1.82. Found: C, 64.12; H, 4.04; N, 1.81. IR: ν_{CO} 1924 (s), 1872 cm^{-1} (m) in CH_2Cl_2. $[Ph_4As]_2[Fe_3(CO)_9(CCO)]$ (III) was synthesized by an analogous procedure. A crystal suitable for X-ray diffraction was obtained by slow diffusion of Et_2O into a CH_2Cl_2 solution of the cluster. Anal. Calcd for $C_{59}H_{40}O_{10}As_2Fe_3$: C, 57.79; H, 3.29. Found: C, 54.65; H, 3.29.

(1) (a) Northwestern University. (b) Recipient of a Gulf Foundation Fellowship. (c) Oklahoma State University.
(2) (a) Bradley, J. S.; Ansell, G. B.; Hill, E. W. *J. Am. Chem. Soc.* **1979**, *101*, 7417. (b) Tachikawa, M.; Muetterties, E. L. *Ibid.* **1980**, *102*, 4541.
(3) (a) Biloen, P.; Sachtler, W. M. H. *Adv. Catal.* **1981**, *30*, 165. (b) Rofer-DePoorter, Ch. K. *Chem. Rev.* **1979**, *79*, 479. (c) Herrmann, W. *Angew. Chem., Int. Ed. Engl.* **1982**, *21*, 117.
(4) Kolis, J. W.; Basolo, F.; Shriver, D. F. *J. Am. Chem. Soc.* **1982**, *104*, 5626.
(5) Holt, E. M.; Whitmire, K. H.; Shriver, D. F. *J. Am. Chem. Soc.* **1982**, *104*, 5621.
(6) Tachikawa, M.; Geerts, R. L.; Muetterties, E. L. *J. Organomet. Chem.* **1981**, *213*, 11.
(7) Kolis, J. W.; Holt, E. M.; Drezdzon, M. A.; Whitmire, K. H.; Shriver, D. F. *J. Am. Chem. Soc.* **1982**, *104*, 6134.
(8) Ceriotti, A.; Chini, P.; Longoni, G.; Piro, G. *Gazz. Chim. Ital.* **1982**, *112*, 353.
(9) Shriver, D. F. "The Manipulation of Air Sensitive Compounds"; McGraw-Hill: New York, 1969.
(10) Hodali, H. A.; Shriver, D. F. *Inorg. Synth.* **1980**, *20*, 222.

0002-7863/83/1505-7307$01.50/0

Table I. Crystal Data for $[Ph_4As][Fe_3(CO)_9(CCO)]$

space group	$P\bar{1}$	V, Å^3	2672.3 (24)
formula	$C_{59}H_{40}As_2Fe_3O_{10}$	$F(000)$	1236
mwt M_r	1226.3	μ(Mo Kα)	21.84
a, Å	10.500 (6)	λ(Mo Kα), Å	0.71069
b, Å	23.789 (14)	D_{calcd}, g cm^{-1}	1.52
c, Å	12.206 (7)	Z	2
α, deg	102.56 (4)	obsd refletns	5538 [$I > 3\sigma(I)$]
β, deg	66.62 (4)	R	8.3%
γ, deg	84.30 (5)		

Synthesis of $[PPN][Fe_3(CO)_{10}(CH)]$ (IV) and $[Ph_4As][Fe_3(CO)_{10}(CH)]$ (V). A 0.5-g sample of either $[PPN]_2[Fe_2(CO)_9(CCO)]$ or $[Ph_4As]_2[Fe_3(CO)_9(CCO)]$ was dissolved in 10 mL of CH_2Cl_2, and then 4 drops of CF_3COOH was added with stirring. The orange solution turned deep red after 10 min, 60 mL of Et_2O was added, and the white precipitate was filtered off. After solvent was removed from the red filtrate under vacuum, the residue was recrystallized from 5 mL of cold (−15 °C) MeOH. Crystals of $[Ph_4As][Fe_3(CO)_{10}(CH)]$ suitable for X-ray diffraction were obtained by slow diffusion of hexane into an Et_2O solution of the cluster. Anal. Calcd for $C_{47}H_{31}NO_{10}P_2Fe_3$: C, 56.49; H, 3.13; N, 1.40. Found: C, 56.45; H, 2.88; N, 1.39. IR: ν_{CO} 1992 (s), 1965 (m), 1940 (sh), 1760 cm^{-1} (m) in MeOH.

Synthesis of $HFe_3(CO)_{10}(CH)$ (VI). A 0.5-g sample of $[PPN]_2[Fe_3(CO)_9(CCO)]$ was dissolved in 10 mL of CH_2Cl_2, and 0.07 mL of CF_3SO_3H was added with stirring. After 10 min, solvent was removed from the blood red solution under vacuum. The red oily solid was extracted with 20 mL of hexane, the solution filtered, and the hexane removed under vacuum. A dry microcrystalline solid was obtained by dissolving the residue in CH_2Cl_2 followed by slow removal of solvent. IR: ν_{CO} 2060 (s), 2053 (vs), 2029 (s), 2011 (m), 1994 cm^{-1} (m) in hexane.

Synthesis of $[PPN][Fe_3(CO)_{10}(CCH_3)]$ (VII). A 0.5-g sample of $[PPN]_2[Fe_3(CO)_9(CCO)]$ was dissolved in 10 mL of CH_2Cl_2, and 0.3 mL of CH_3I was added with stirring. The solution turned red instantly and after 20 min 60 mL of Et_2O was added. The resulting white solid was filtered off and solvent removed under vacuum from the red filtrate. The oil was redissolved in 10 mL of MeOH and crystallized overnight at −10 °C. Anal. Calcd for $C_{48}H_{33}NO_{10}P_2Fe_3$: C, 56.90; H, 3.28; N, 1.38. Found: C, 57.14; H, 3.45; N, 1.70. IR: ν_{CO} 1989 (s), 1965 (s), 1944 (m), 1934 (sh), 1911 (m), 1679 cm^{-1} (m) in MeOH.

^{13}C Enrichment of $[PPN]_2[Fe_3(CO)_{11}]$ and $[PPN]_2[Fe_3(CO)_9(CCO)]$. A 1.0-g sample of $[PPN]_2[Fe_3(CO)_{11}]$ was dissolved in 20 mL of CH_3CN. The solution was degassed, and 360 torr of ^{13}CO was placed over the solution, which was then stirred for 1 h at 25 °C. The exchanged CO was removed, the solution exposed to fresh ^{13}CO, and the process repeated. After filtration to remove an unidentified orange solid, the CH_3CN was removed under vacuum. This procedure results in ~25% enrichment of all carbonyls in $[Fe_3(CO)_{11}]^{2-}$, and acylation followed by reductive cleavage results in the production of $[Fe_3(CO)_9(CCO)]^{2-}$ that has been enriched at all carbon atoms.

Selective enrichment of $[PPN]_2[Fe_3(CO)_9(CCO)]$ was accomplished by dissolving 0.8 g of the cluster in 15 mL of CH_3CN in a 100-mL gas bulb and stirring with 1 atm of ^{13}CO for 24 h. This process enriched the CO ligands to approximately 12% ^{13}C.

X-ray Crystallography of $[Ph_4As]_2[Fe_3(CO)_9(CCO)]$. A crystal of III was fixed in a capillary under N_2 and mounted on a Syntex P3 automated diffractometer. Unit cell dimensions (Table I) were determined by least-squares refinement of the best angular positions for 15 independent reflections ($2\theta > 15°$) during normal alignment procedures using Mo radiation ($\lambda = 0.71069$ Å). A total of 12900 data points were collected at room temperature by using a variable scan rate, a θ–2θ scan mode, and a scan width of 1.2° below Kα_1 and 1.2° above Kα_2 to a maximum 2θ value of 116°. The background was measured on each side of the scan for a combined time equal to the total scan time. The intensities of three standard reflections were remeasured after every 97 reflections; since the intensities of these reflections showed less than 8% variation, corrections for decomposition were deemed unnecessary. Data were corrected for Lorentz, polarization, and background effects. After removal of redundant and space group forbidden data, 3535 reflections were considered observed [$I > 3.0\sigma(I)$]. The structure was solved by direct methods using MULTAN80.[11] Refinement of scale factor and positional and anisotropic thermal parameters for all non-hydrogen atoms was carried out to convergence.[12] Hydrogen positional parameters were not determined. The

(11) Main, P.; Fiske,; Hull, S. E.; Lessinger, L.; Germain, G.; DeClerq, J. P.; Woolfson, M. M. "MULTAN80"; University of York, England, 1980.
(12) Stewart, J. M., Ed. "The X-Ray System-Version of 1980"; Technical Report TR446 of the Computer Center, University of Maryland, College Park, MD.

Table II. Positional Parameters for $[Ph_4As][Fe_3(CO)_9(CCO)]$[a]

atom	x (sig(x))	y (sig(y))	z (sig(z))
Fe1	0.5512 (3)	0.1935 (1)	0.6528 (2)
Fe2	0.5661 (3)	0.2618 (1)	0.8409 (2)
Fe3	0.3249 (3)	0.2437 (1)	0.8513 (2)
As1	0.1288 (2)	0.0826 (1)	0.1539 (2)
As2	0.9157 (2)	0.4419 (1)	0.2976 (2)
C998	0.4865 (18)	0.1892 (8)	0.8220 (17)
C999	0.5543 (18)	0.1653 (9)	0.8730 (16)
O999	0.6086 (17)	0.1387 (7)	0.9193 (16)
C11	0.5302 (21)	0.2415 (8)	0.5735 (19)
O11	0.5206 (16)	0.2759 (6)	0.5167 (13)
C12	0.7375 (26)	0.1663 (10)	0.5681 (18)
O12	0.8563 (17)	0.1476 (8)	0.5096 (15)
C13	0.4935 (25)	0.1339 (9)	0.5826 (22)
O13	0.4599 (21)	0.0947 (7)	0.5357 (16)
C21	0.7531 (22)	0.2424 (11)	0.7836 (21)
O21	0.8747 (16)	0.2304 (8)	0.7475 (17)
C22	0.5151 (22)	0.2933 (9)	1.0003 (17)
O22	0.4841 (19)	0.3159 (7)	1.1036 (13)
C23	0.5466 (23)	0.3256 (8)	0.7910 (18)
O23	0.5417 (19)	0.3677 (6)	0.7623 (15)
C31	0.2239 (23)	0.2653 (10)	1.0131 (21)
O31	0.1572 (18)	0.2804 (8)	1.1191 (15)
C32	0.2176 (23)	0.1986 (11)	0.8093 (20)
O32	0.1488 (19)	0.1709 (9)	0.7766 (18)
C33	0.2694 (23)	0.3056 (11)	0.8138 (25)
O33	0.2308 (19)	0.3497 (8)	0.7980 (20)
C111	0.0435 (19)	0.0312 (7)	0.2416 (17)
C112	0.1256 (24)	−0.0087 (9)	0.2726 (20)
C113	0.0655 (34)	−0.0498 (10)	0.3312 (24)
C114	−0.0772 (37)	−0.0505 (12)	0.3627 (21)
C115	−0.1565 (33)	−0.0125 (13)	0.3326 (22)
C116	−0.1015 (24)	0.0297 (9)	0.2742 (19)
C121	0.2084 (16)	0.1305 (7)	0.2442 (16)
C122	0.2931 (20)	0.1672 (9)	0.1878 (20)
C123	0.3532 (21)	0.2029 (9)	0.2574 (23)
C124	0.3266 (21)	0.1989 (9)	0.3764 (20)
C125	0.2377 (22)	0.1641 (8)	0.4337 (20)
C126	0.1767 (20)	0.1309 (9)	0.3671 (18)
C131	0.2727 (18)	0.0401 (8)	−0.0077 (15)
C132	0.3353 (20)	0.0712 (8)	−0.0919 (17)
C133	0.4398 (21)	0.0372 (9)	−0.2118 (16)
C134	0.4793 (22)	−0.0247 (9)	−0.2421 (18)
C135	0.4142 (24)	−0.0527 (9)	−0.1558 (22)
C136	0.3084 (20)	−0.0224 (9)	−0.0347 (18)
C141	−0.0104 (16)	0.1287 (6)	0.1297 (15)
C142	−0.1033 (22)	0.1776 (9)	0.2305 (19)
C143	−0.2092 (24)	0.2095 (10)	0.2127 (22)
C144	−0.2234 (22)	0.1939 (10)	0.1027 (22)
C145	−0.1316 (20)	0.1459 (9)	0.0064 (19)
C146	−0.0254 (21)	0.1166 (7)	0.0201 (18)
C211	0.8840 (30)	0.4099 (10)	0.1567 (23)
C212	0.8786 (24)	0.3511 (9)	0.1209 (18)
C213	0.8567 (27)	0.3320 (10)	0.0133 (22)
C214	0.8408 (44)	0.3658 (14)	−0.0504 (34)
C215	0.8631 (71)	0.4197 (19)	−0.0291 (47)
C216	0.8699 (65)	0.4458 (16)	0.0864 (44)
C221	0.9398 (21)	0.3845 (7)	0.3778 (16)
C222	0.8284 (19)	0.3538 (9)	0.4278 (17)
C223	0.8465 (24)	0.3127 (8)	0.4881 (18)
C224	0.9736 (23)	0.3013 (8)	0.4977 (18)
C225	1.0848 (23)	0.3312 (8)	0.4461 (20)
C226	1.0644 (20)	0.3716 (9)	0.3879 (17)
C231	1.0855 (22)	0.4709 (7)	0.2393 (16)
C232	1.0943 (20)	0.5252 (8)	0.2989 (17)
C233	1.2247 (24)	0.5443 (9)	0.2535 (19)
C234	1.3455 (28)	0.5086 (11)	0.1553 (22)
C235	1.3357 (28)	0.4535 (12)	0.0960 (22)
C236	1.2050 (26)	0.4336 (9)	0.1376 (19)
C241	0.7652 (23)	0.5075 (10)	0.4159 (23)
C242	0.7302 (32)	0.5501 (13)	0.3730 (32)
C243	0.6306 (37)	0.6036 (14)	0.4604 (44)
C244	0.5507 (30)	0.6003 (13)	0.5785 (33)
C245	0.5869 (32)	0.5586 (14)	0.6183 (24)
C246	0.6890 (30)	0.5049 (12)	0.5355 (21)

[a] Standard deviations are given in units of the last significant figure.

Table III. Crystal Data for $[Ph_4As][Fe_3(CO)_{10}(CH)]$

space group	$P\bar{1}$	V, Å^3	1692.7 (27)
formula	$AsFe_3C_{35}H_{21}O_{10}$	$F(000)$	844.0
mwt M_r	843.4	μ(Mo Kα)	24.15
a, Å	15.527 (8)	λ(Mo Kα), Å	0.71069
b, Å	7.764 (3)	D_{calcd}, g cm^{-1}	1.67
c, Å	14.687 (20)	Z	2
α, deg	85.48 (8)	obsd reflctns	5087
β, deg	74.37 (9)	R	8.0%
γ, deg	93.81 (3)		

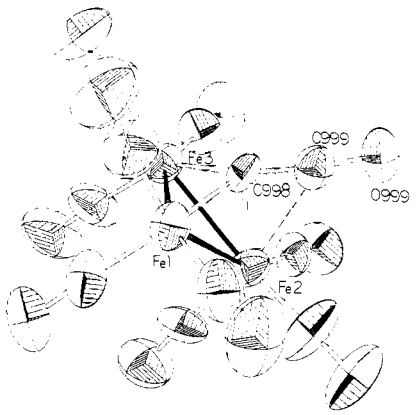

Figure 1. ORTEP drawing of the ketenylidene cluster dianion $[Fe_3(CO)_9(CCO)]^{2-}$ (III).

final cycle of refinement [function minimized $\sum(|F_o| - |F_c|)^2$] led to a final agreement factor, R, of 8.3%. [$R = ((\sum||F_o| - |F_c||)/|F_o|) \times 100$]. Anomalous dispersion corrections were made for Fe and As. Scattering factors were taken from Cromer and Mann.[13] Unit weights were used throughout. The positional parameters are listed in Table II.

X-ray Crystallography of $[Ph_4As][Fe_3(CO)_{10}(CH)]$. A crystal of V was sealed in a capillary under N_2. Details of the unit cell determination (Table III), data collection, and corrections to the data, methods of solution, and computer programs are identical with those described above. A total of 13 049 data points were obtained at room temperature; of these 5087 reflections were considered observed [$I > 3.0\sigma(I)$]. Refinement of scale factor and positional and anisotropic thermal parameters for all non-hydrogen atoms was carried out to convergence.[12] Hydrogen positional parameters for phenyl hydrogens were calculated by assuming normal geometry and a C–H distance of 0.97 Å. H998 was located from a difference Fourier synthesis. These hydrogen positional parameters were included in the final cycles of refinement. The hydrogen atoms were assigned isotropic thermal parameters of $U = 0.03$. All parameters associated with hydrogen atoms in the phenyl groups were held invariant. The final cycle of refinement led to the agreement factor $R = 8.0\%$. The positional parameters are listed in Table IV.

Results and Discussion

Structure of $[Ph_4As]_2[Fe_3(CO)_9(CCO)]$ (III). This compound exists in the solid state as a well-separated cation and dianion cluster with no interionic contact distances of less than 3 Å (Table V). The tetraphenylarsonium groups show normal tetrahedral bonding of arsenic to phenyl groups, and all angles and distances for these clusters are reasonable. The iron carbonyl cluster displays a nearly equilateral arrangement of iron atoms (average Fe–Fe of 2.564 (4) Å), and each iron atom is coordinated to three terminal carbonyl groups [average Fe–C bond distance 1.76 (2) Å, average C–O distance 1.15 (3) Å, Fe–C–O angles 174.1 (21)–179.1 (28)°]. The CCO group is only approximately linear, C998–C999–0999 = 172.8 (23)°, and is not perpendicular to the plane of the three iron atoms as evidenced by the range of Fe–C990–C99 angles [Fe], 129.6 (12)°; Fe2, 92.2 (15)°; Fe3, 145.0 (14)°] and also by the 33.49° between the "best" line through C998–C999–0999 (std dev 0.04) and the perpendicular to the plane of the iron atoms (Figure 1). The three Fe–C998 distances are not equal (Fe1–C998, 1.93 (2) Å; Fe2–C998, 2.00 (2) Å; Fe3–C998, 1.89 (2) Å, and Fe2 (toward which the CCO is tilted) is 2.42 (2) Å from the central carbon of the ketenylidene ligand. This distance is long for an iron–carbon bonding distance and shorter than the usual nonbonding distance. Oxygen 999 is bent away from Fe2. $[PPN][Fe_4(CO)_{11}(\mu\text{-CO})(\mu_3\text{-COCH}_3)]$ displays

(13) Cromer, D. T.; Mann, I. B. *Acta Crystallogr., Sect. A* **1968**, *A2*, 321.

Table IV. Positional Parameters for $[Ph_4As][Fe_3(CO)_9(\mu\text{-CO})(CH)]$

atom	x (sig(x))	y (sig(y))	z (sig(z))
Fe1	0.3164 (1)	0.4041 (2)	−0.1894 (1)
Fe2	0.1485 (1)	0.3290 (3)	−0.1670 (1)
Fe3	0.2566 (1)	0.3295 (3)	−0.3292 (1)
C11	0.3294 (8)	0.6378 (17)	−0.1965 (9)
C12	0.4267 (9)	0.3521 (18)	−0.2411 (10)
C13	0.3150 (9)	0.3509 (17)	−0.0705 (10)
C21	0.1353 (9)	0.4956 (20)	−0.0888 (9)
C22	0.0438 (10)	0.3070 (20)	−0.1929 (12)
C23	0.1230 (10)	0.1398 (20)	−0.0836 (12)
C31	0.3161 (13)	0.1493 (23)	−0.3663 (11)
C32	0.1825 (10)	0.2958 (19)	−0.3988 (10)
C33	0.3376 (11)	0.4956 (20)	−0.3948 (11)
C34	0.1854 (9)	0.5104 (21)	−0.2751 (10)
C998	0.2539 (9)	0.2036 (17)	−0.2087 (8)
O11	0.3382 (8)	0.7874 (14)	−0.1986 (8)
O12	0.4966 (7)	0.3128 (16)	−0.2702 (9)
O13	0.3196 (8)	0.3100 (14)	−0.0040 (7)
O21	0.1219 (8)	0.6016 (15)	−0.0392 (7)
O22	−0.0231 (7)	0.2954 (16)	−0.2103 (10)
O23	0.1068 (8)	0.0224 (16)	−0.0310 (9)
O31	0.3560 (9)	0.0343 (17)	−0.3929 (8)
O32	0.1364 (8)	0.2694 (17)	−0.4455 (9)
O33	0.3874 (8)	0.6016 (16)	−0.4444 (8)
O34	0.1717 (8)	0.6571 (15)	−0.2936 (8)
As1	0.2529 (1)	0.4724 (2)	0.2594 (1)
C111	0.1554 (8)	0.3282 (15)	0.2436 (9)
C112	0.1193 (9)	0.3673 (17)	0.1691 (10)
C113	0.0452 (10)	0.2606 (20)	0.1642 (12)
C114	0.0106 (9)	0.1239 (20)	0.2305 (12)
C115	0.0486 (10)	0.0836 (19)	0.3026 (11)
C116	0.1217 (9)	0.1854 (17)	0.3072 (10)
C121	0.3076 (8)	0.6316 (15)	0.1506 (8)
C122	0.3972 (8)	0.6248 (17)	0.0999 (9)
C123	0.4328 (10)	0.7460 (21)	0.0234 (10)
C124	0.3851 (12)	0.8676 (22)	−0.0024 (10)
C125	0.2979 (11)	0.8767 (20)	0.0472 (11)
C126	0.2572 (10)	0.7550 (17)	0.1242 (10)
C131	0.2107 (9)	0.6099 (15)	0.3601 (9)
C132	0.2689 (10)	0.7233 (20)	0.3847 (11)
C133	0.2387 (11)	0.8267 (21)	0.4574 (12)
C134	0.1491 (10)	0.8184 (19)	0.5025 (9)
C135	0.0907 (10)	0.7136 (20)	0.4740 (11)
C136	0.1196 (9)	0.6055 (18)	0.4035 (9)
C141	0.3352 (8)	0.3216 (16)	0.2850 (8)
C142	0.3588 (9)	0.1908 (19)	0.2254 (9)
C143	0.4200 (10)	0.0781 (20)	0.2399 (11)
C144	0.4563 (10)	0.0932 (21)	0.3132 (12)
C145	0.4348 (10)	0.2227 (22)	0.3720 (11)
C146	0.3726 (9)	0.3373 (18)	0.3586 (9)
H998	0.266 (7)	0.076 (14)	−0.193 (7)
H112	0.1452	0.4691	0.1215
H113	0.0186	0.2862	0.1102
H114	−0.0432	0.0519	0.2274
H115	0.0222	−0.0184	0.3511
H116	0.1515	0.1551	0.3582
H122	0.4333	0.5350	0.1191
H123	0.4963	0.7437	−0.0139
H124	0.4133	0.9520	−0.0590
H125	0.2639	0.9704	0.0271
H126	0.2543	0.8237	0.1791
H132	0.3339	0.7313	0.3506
H133	0.2820	0.9041	0.4770
H134	0.1270	0.8900	0.5545
H135	0.0253	0.7129	0.5042
H136	0.0760	0.5276	0.3841
H142	0.3307	0.1804	0.1724
H143	0.4381	−0.0120	0.1962
H144	0.4988	0.0100	0.3251
H145	0.4636	0.2342	0.4236
H146	0.3546	0.4289	0.4023

Table V. Cluster Distances (Å) and Bond Angles (deg) for $[Ph_4As]_2[Fe_3(CO)_9(CCO)]$

Fe1-Fe2	2.579 (4)	Fe1-Fe2-Fe3	59.6 (1)
Fe1-Fe3	2.560 (3)	Fe2-Fe3-Fe1	60.4 (1)
Fe2-Fe3	2.569 (5)	Fe3-Fe1-Fe2	60.0 (1)
Fe1-C11	1.70 (2)	Fe1-C998-C999	129.6 (12)
Fe1-C12	1.78 (2)	Fe2-C998-C999	92.2 (15)
Fe1-C13	1.78 (2)	Fe3-C998-C999	145.0 (14)
Fe2-C21	1.77 (2)	C998-C999-O999	172.8 (23)
Fe2-C22	1.76 (2)	Fe1-C11-O11	177.3 (21)
Fe2-C23	1.78 (2)	Fe1-C12-O12	177.2 (22)
Fe3-C31	1.75 (2)	Fe1-C13-O13	178.2 (20)
Fe3-C32	1.77 (3)	Fe2-C21-O21	179.1 (25)
Fe3-C33	1.75 (3)	Fe2-C22-O22	174.1 (21)
Fe1-C998	1.93 (2)	Fe2-C23-O23	174.7 (25)
Fe2-C998	2.00 (2)	Fe3-C31-O31	178.8 (24)
Fe3-C998	1.89 (2)	Fe3-C32-O32	176.0 (26)
Fe2-C999	2.42 (2)	Fe3-C33-O33	174.5 (25)
C998-C999	1.28 (3)		
C999-O999	1.18 (3)	Fe2-C999-C998	55.8 (12)
C11-O11	1.20 (3)		
C12-O12	1.14 (3)		
C13-O13	1.15 (3)		
C21-O21	1.15 (3)		
C22-O22	1.15 (2)		
C23-O23	1.13 (3)		
C31-O31	1.15 (3)		
C32-O32	1.15 (4)		
C33-O33	1.17 (4)		

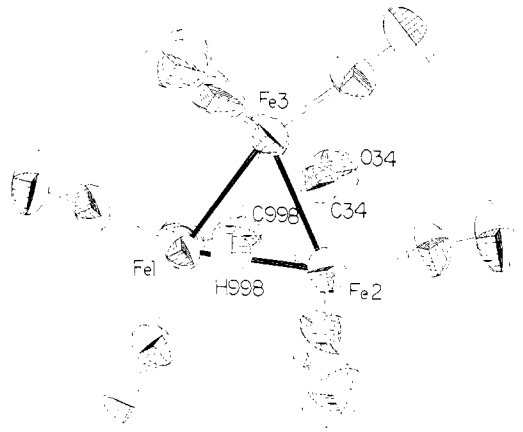

Figure 2. ORTEP drawing of the triiron methyne cluster anion $[Fe_3(CO)_{10}(CH)]^-$.

a slightly bridging carbonyl group where the bending of the carbonyl group (Fe–C–O = 164 (3)°) appears to arise from the approach (2.45 (4) Å) of another iron atom.[14] However, in this case the tetrahedral cluster has a normal 60-electron count and the carbonyl functions as a two-electron donor in both bridging and terminal orientations.

By contrast, the ketenylidene ligand in the isoelectronic osmium cluster $(\mu\text{-H})_2Os_3(CO)_9(\mu_3\text{-CCO})$ is perpendicular to the plane of the three osmium atoms.[15] All three osmium–ketenylidene carbon distances fall in the range 2.157 (26) – 2.133 (20) Å. Despite the differences in geometry, the C–C distance, 1.264 (37) Å, and C–O distance, 1.154 (34) Å, are similar to those observed here [C998–C999, 1.28 (3), C999–O999, 1.18 (3) Å].

Structure of $[Ph_4As][Fe_3(CO)_9(\mu\text{-CO})(\mu_3\text{-CH})]$ (V). This compound crystallizes in a unit cell with one anionic iron cluster and one cation per asymmetric unit, in contrast to a previous determination with PPN^+ as the charge balancing cation, in which two iron clusters and two cationic groups comprise the asymmetric unit. In the previous structure determination, one of the two iron clusters refined satisfactorily and the second displayed considerable disorder.[7] The general structure of the iron cluster in the present more precise determination is consistent with that of the ordered cluster in the previous work (Table VI). The three iron atoms form an approximately equilateral triangle of average Fe–Fe distance (2.548 (4) Å), with the edge bridged by the carbonyl (Fe2–Fe3) being the shortest (2.518 (4) Å) (Figure 2). The carbonyl bridge is symmetric [Fe2–C34, 1.95 (1) Å; Fe3–C34, 1.94 (2) Å], and the C–O distance (1.19 Å) is slightly larger than the C–O average distance (1.14 (2) Å) for the other nine terminal carbonyl groups.

Carbon C998 of the methylidyne is approximately symmetrically disposed in a μ_3 bridge, with slightly larger Fe–C distances to the two iron atoms also bridged by a CO group [Fe2–C998,

Table VI. Distances (Å) and Bond Angles (deg) for $[Ph_4As][Fe_3(CO)_9(\mu\text{-CO})(CH)]$

Fe1-Fe2	2.557 (3)	Fe1-Fe2-Fe3	60.83 (9)
Fe2-Fe3	2.518 (4)	Fe2-Fe3-Fe1	60.34 (11)
Fe1-Fe3	2.569 (4)	Fe3-Fe1-Fe2	58.83 (9)
Fe1-C11	1.80 (1)	Fe1-C998-H998	127 (7)
Fe1-C12	1.77 (1)	Fe2-C998-H998	132 (5)
Fe1-C13	1.75 (1)	Fe3-C998-H998	129 (6)
Fe2-C21	1.80 (2)		
Fe2-C22	1.77 (2)	Fe1-C11-O11	178.1 (13)
Fe2-C23	1.77 (2)	Fe1-C12-O12	176.5 (13)
Fe2-C34	1.95 (1)	Fe1-C13-O13	174.9 (13)
Fe3-C31	1.78 (2)	Fe2-C21-O21	176.1 (13)
Fe3-C32	1.76 (2)	Fe2-C22-O22	179.0 (13)
Fe3-C33	1.75 (1)	Fe2-C23-O23	179.4 (21)
Fe3-C34	1.94 (2)	Fe2-C34-O34	138.0 (11)
		Fe3-C31-O31	178.2 (14)
Fe1-C998	1.86 (1)	Fe3-C32-O32	177.4 (14)
Fe2-C998	1.95 (1)	Fe3-C33-O33	173.7 (16)
Fe3-C998	1.93 (1)	Fe3-C34-O34	141.4 (10)
C11-O11	1.16 (2)	C111-As1-C121	112.4 (5)
C12-O12	1.13 (2)	C111-As1-C131	109.9 (5)
C13-O13	1.13 (2)	C111-As1-C141	106.0 (5)
C21-O21	1.14 (2)	C121-As1-C131	105.7 (5)
C22-O22	1.13 (2)	C121-As1-C141	110.6 (5)
C23-O23	1.10 (2)	C131-As1-C141	112.3 (6)
C31-O31	1.16 (2)		
C32-O32	1.14 (2)	As1-C111-C112	121.0 (8)
C33-O33	1.14 (2)	As1-C111-C116	118.8 (11)
C34-O34	1.19 (2)	C111-C112-C113	118.0 (12)
		C112-C113-C114	120.6 (16)
C998-H998	1.04 (11)	C113-C114-C115	120.8 (15)
		C114-C115-C116	118.9 (13)
As1-C111	1.90 (1)	C115-C116-C111	121.3 (15)
As1-C121	1.88 (1)	C116-C111-C112	120.2 (12)
As1-C131	1.90 (1)	As1-C121-C122	120.7 (9)
As1-C141	1.88 (1)	As1-C121-C126	117.9 (8)
		C121-C122-C123	117.5 (13)
C111-C112	1.38 (2)	C122-C123-C124	121.8 (13)
C112-C113	1.39 (2)	C123-C124-C125	121.2 (14)
C113-C114	1.34 (2)	C124-C125-C126	119.8 (16)
C114-C115	1.36 (2)	C125-C126-C121	118.2 (13)
C115-C116	1.36 (2)	C126-C121-C122	121.4 (10)
C116-C111	1.35 (2)		
C121-C122	1.40 (2)	As1-C131-C132	120.4 (9)
C122-C123	1.36 (2)	As1-C131-C136	120.0 (10)
C123-C124	1.32 (2)	C131-C132-C133	121.0 (13)
C124-C125	1.36 (2)	C132-C133-C134	119.6 (16)
C125-C126	1.38 (2)	C133-C134-C135	119.3 (14)
C126-C121	1.37 (2)	C134-C135-C136	122.0 (13)
		C135-C136-C131	118.5 (13)
C131-C132	1.36 (2)	C136-C131-C132	119.4 (12)
C132-C133	1.40 (2)	As1-C141-C142	118.1 (10)
C133-C134	1.36 (2)	As1-C141-C146	121.8 (10)
C134-C135	1.35 (2)	C141-C142-C143	120.6 (14)
C135-C136	1.39 (2)	C142-C143-C144	119.1 (15)
C136-C131	1.38 (2)	C143-C144-C145	121.2 (16)
		C144-C145-C146	120.4 (16)
C141-C142	1.41 (2)	C145-C146-C141	118.5 (13)
C142-C143	1.38 (2)	C146-C141-C142	120.1 (12)
C143-C144	1.35 (3)		
C144-C145	1.39 (2)		
C145-C146	1.40 (2)		
C146-C141	1.37 (2)		

(14) Holt, E. M.; Whitmire, K. H.; Shriver, D. F. *J. Chem. Soc., Chem. Commun.* **1980**, 778.
(15) Shapley, J. R.; Strickland, D. S.; St. George, G. M.; Churchill, M. R.; Bueno, C. *Organometallics* **1983**, *2*, 185.

Table VII

compound	^{1}H NMR ppm	^{13}C NMR[e] ppm	ref
$[Fe_3(CO)_9(CCO)]^{2-}$ [b]		222.3, 182.2, 90.1; J(CC) = 74 Hz	*a*
$[Fe_3(CO)_{10}(CH)]^-$ [b]	12.24	262.4, 220.5; J(CH) = 165 Hz	*a*
$[Fe_3(CO)_{10}CH^-$ [c]	12.16, −20.52	264.0, 207.8 (4), 206.6 (3), 204.7 (3); J(CH) = 168 Hz	*a*
$[Fe_3(CO)_{10}CCH_3]^-$ [b]	4.06	286.2, 221.2, 43.6	*a*, 23
$H_2Os_3(CO)_9(CCO)$	−19.73	175.6, 165.8, 160.3, 8.6; J(CC) = 86 Hz	22
$H_3Fe_3(CO)_9CCH_3$	4.33, −23.55	206.4, 46.2 (*d*)	24

[a] This work. [b] CD_3CN at −40 °C. [c] toluene-d_8 at −50 °C. [d] Quaternary carbon not observed. [e] All resonances in ppm downfield from Me_4Si.

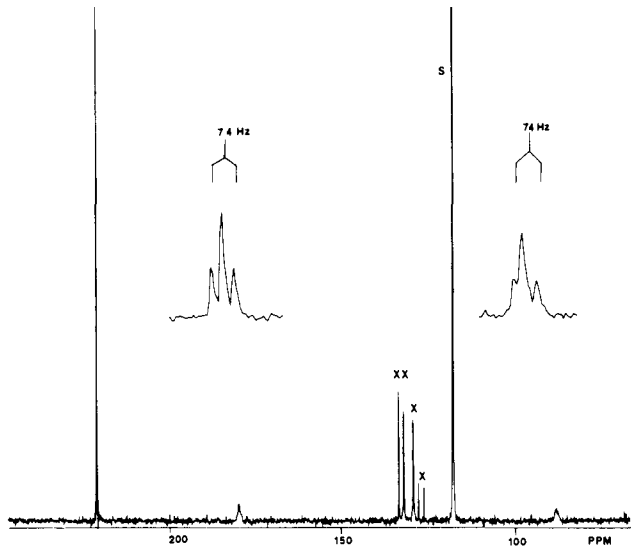

Figure 3. 67.8-MHz ^{13}C NMR spectrum of $[PPN]_2[Fe_3(CO)_9(CCO)]$ (II) in CD_3CN at −40 °C. The expanded views of the two carbon resonances of the ketenylidene clearly show the satellites due to carbon–carbon coupling. X resonances due to PPN; S, acetonitrile solvent.

1.95 (1) Å; Fe3–C998, 1.93 Å] than to the unique iron atom [Fe1–C998, 1.86 (1) Å].

In contrast to the previous structural determination, the methylidyne hydrogen could be located in the present work from inspection of the difference Fourier map and refinement of its position. The hydrogen appears to be slightly skewed with respect to the iron triangle (angle 3.98° between the C–H bond and perpendicular to the plane of the three iron atoms that passes through C998) as evidenced by the differences in the three nonbonding Fe–H998 distances [Fe1–H9, 2.625 (2) Å; Fe2–H998, 2.752 (2) Å; Fe–H998, 2.704 (3) Å]. The hydrogen atom shows two close contact distances with C23 and C31 [2.48 (1) and 2.47 (1) Å, respectively], but is clearly terminal. It is thus fundamentally different from $HFe_4(CO)_{12}(\mu_4\text{-}CH)$,[16] in which the C–H serves as a 5-electron donor to a 62-electron butterfly cluster with Fe–C distances 1.946 (5) Å and 1.939 (4) Å to the "hinge" iron atoms, 1.828 (5) Å to the "wing" iron atom, and 1.926 (5) Å to the iron atom involved in the three center bond [Fe–H, 1.80 (4) Å]. Further interpretation of the hydrogen position in the structure determined here is limited by the realization that single-crystal X-ray data do not allow accurate determination of hydrogen positions despite their apparent stability to refinement.

The structure of the three-iron methylidyne cluster is also distinctly different from that observed for $(\mu\text{-}H)Os_3(CO)_{10}(\mu_3\text{-}CH)$[17] in which the μ_3 bonding to an isosceles triangle of osmium atoms [Os2–Os3, 2.910 (1) Å; Os1–Os3, 2.845 (1) Å; Os1–Os2, 2.842 (1) Å] is clearly asymmetric [Cl–Os1, 2.353 (10) Å; Cl–Os2, 2.003 (11) Å; Cl–Os3, 2.011 (12) Å]. In that cluster, the C–H hydrogen shows a pronounced tilt toward Os1 [H1–Os1], 2.36 (14) Å] and also displays a close contact (1.81 (14) Å) with the carbon of a terminal carbonyl attached to this osmium atom. Comparison may also be made with the cationic rhodium cluster $[(\mu_5\text{-}C_5H_5)_3Rh_3(\mu\text{-}CO)_2(\mu_3\text{-}CH)]^+$, in which an equilateral rhodium triangle binds a methylidyne group in symmetric μ_3-fashion (Rh–C methylidyne distances showing a 0.036-Å range) with the C–H bond virtually perpendicular to the plane of the rhodium triangle.[18]

Chemistry and Spectroscopy. $Fe_3(CO)_9(CCO)^{2-}$ is easily synthesized in high yield by the reductive cleavage of an activated C–O bond followed by, or simultaneous with, the migration of a carbon monoxide from the metal framework onto the exposed carbide atom to form a ketenylidene (eq 2). Although we believe

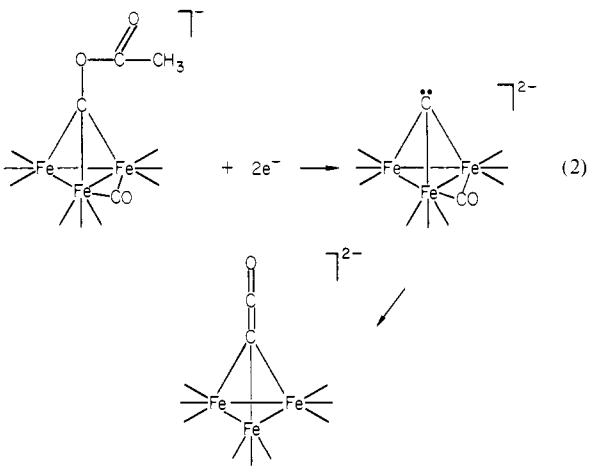

(2)

it is less likely, intermolecular CO transfer cannot be discounted. Migration of CO onto a carbide has been proposed before for carbide type species[2a,19] and recently for an exposed nitride.[20] As described below, ^{13}C NMR spectroscopy indicates the existence of the ketenylidene functionality, and the spectral parameters are in good agreement with those reported previously[21] for the isoelectronic $H_2Os_3(CO)_9(CCO)$[21] (Table VII). When ^{13}C NMR spectroscopy is performed on $[Fe_3(CO)_9(CCO)]^{2-}$ which has been enriched on all carbon atoms, the low-field shift characteristic of a carbide atom is not observed. However, resonances at 181 and 90 ppm clearly display ^{13}C satellites (Figure 3). The carbon–carbon coupling constant of 74 Hz is similar to that of a C=C double bond and is slightly less than that in $H_2Os_3(CO)_9(CCO)$. When an unenriched sample of II is stirred under an atmosphere of ^{13}CO overnight, both the terminal carbonyls and the kete-

(16) Beno, M. A.; Williams, J. M.; Tachikawa, M.; Muetterties, E. L. *J. Am. Chem. Soc.* **1980**, *102*, 4542.

(17) Shapley, J. R.; Cree-Uchiyama, M. E.; St. George, G. M.; Churchill, M. R.; Bueno, C. *J. Am. Chem. Soc.* **1983**, *105*, 140.

(18) (a) Dimas, P. A.; Duesler, E. N.; Lawson, R. J.; Shapley, J. R. *J. Am. Chem. Soc.* **1980**, *102*, 7787. (b) Herrmann, W. A.; Plank, J.; Riedel, D.; Ziegler, M. L.; Weidenhammer, K.; Guggolz, E.; Balbach, B. *Ibid.* **1981**, *103*, 63.

(19) (a) Seyferth, D.; Hallgren, J. E.; Eschbach, C. S. *J. Am. Chem. Soc.* **1974**, *96*, 1730. (b) Davis, J. H.; Beno, M. A.; Williams, J. M.; Zimmie, J.; Tachikawa, M.; Muetterties, E. L. *Proc. Natl. Acad. Sci. USA* **1981**, *78*, 668.

(20) (a) Blohm, M. L.; Fjare, D. E.; Gladfelter, W. L. *Inorg. Chem.* **1983**, *22*, 1004. (b) Herrmann, W. A.; Bell, L. K.; Ziegler, M. L.; Pfisterer, H.; Pahl, C. *J. Organomet. Chem.* **1983**, *247*, 39.

(21) (a) Sievert, A. C.; Strickland, D. S.; Shapley, J. R.; Steinmetz, G. R.; Geoffroy, G. L. *Organometallics* **1982**, *1*, 214. (b) Arce, A. J.; Deeming, A. J. *J. Chem. Soc., Chem. Commun.* **1982**, 364.

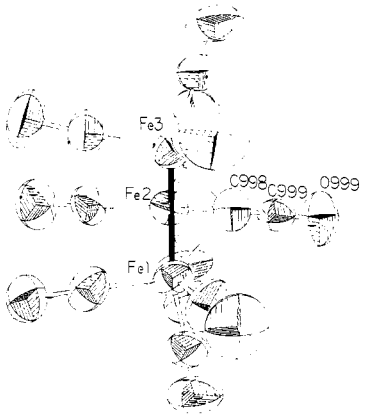

Figure 4. Drawing of the $[Fe_3(CO)_9(CCO)]^{2-}$ cluster showing how the CO's are arrayed so as to allow easy access to the coordinated carbon of the ketenylidene.

nylidene undergo CO exchange, as shown by the presence of singlets at 181 and 222 ppm and lack of a resonance around 90 ppm in the ^{13}C NMR. However, the peaks characteristic of CO bound to carbon and CO bound to iron do not coalesce even at 50 °C, so intramolecular exchange is slow on the NMR time scale.

The tilt of the CCO ligand may facilitate reactions at the α carbon of this ligand. Figure 4 indicates that this tilt results in an open channel, which may make the α carbon accessible to attack. (Even relatively weak acids such as CH_3COOH react instantly with the cluster.) Protonation of the α–C of the ketenylidene results in displacement of the CO onto the metal framework (eq 3). This process may be facilitated by the close

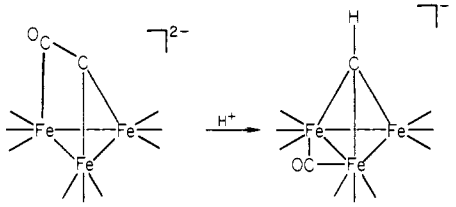

(3)

proximity of the ketenyl CO to Fe2 of the metal cluster, which results from tilt of the ketenylidene ligand. The ^1H NMR spectrum displays a peak at 12.24 ppm, typical of a methylidyne proton, and the ^{13}C NMR spectrum shows a doublet centered at 262.4 ppm (J_{C-H} = 165 Hz). Selective irradiation of the proton resonance at 12.24 ppm causes the doublet to collapse to a singlet in the ^{13}C spectrum, confirming the attachment of the proton to the apical carbon (Table VII).

As determined by NMR, further protonation of the cluster with a strong acid results in the placement of a hydride across a Fe–Fe bond (eq 4) with no substantial shifts in the other resonance (Table

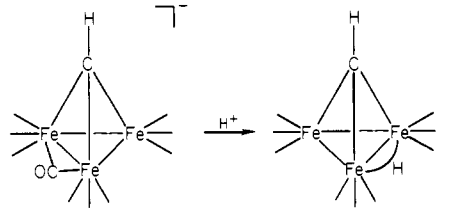

(4)

VII). Neither the IR nor the ^{13}C NMR spectrum indicates the presence of a bridging CO, but the resonances in the terminal CO region of the ^{13}C NMR are of intensities 4:3:3, suggesting that the C–H is not symmetrically disposed.

The methylidyne proton in the monoanion exchanges at a moderate rate with protic solvents. Thus, acetone-d_6, in the proton resonance disappears over ~1 h, and the doublet in the ^{13}C spectrum disappears with concomitant appearance of a triplet due to coupling of the deuteron (J_{C-D} = 26 Hz). The exchange reaction is acid catalyzed, so one drop of acetic acid added to the

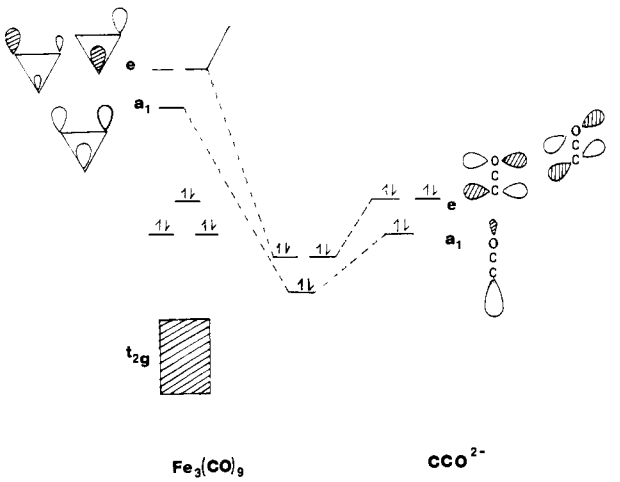

Figure 5. Energy level diagram illustrating the interaction between the three highest filled orbitals of the $(CCO)^{2-}$ ligand with the three low-lying acceptor orbitals of identical symmetry of the $Fe_3(CO)_9$ fragment. (The $Fe_3(CO)_9$ orbitals were taken from ref 25. The CCO^{2-} orbitals were determined using standard extended Hückel techniques.) The energy levels are approximate.

NMR tube causes complete exchange within time of measurement.

The coordinated carbon is susceptible to attack by other electrophiles as well. For example, it reacts almost immediately with methyl iodide to yield the ethylidyne, with the migration of the ketenylidyne CO to the metal cluster framework (eq 5). This

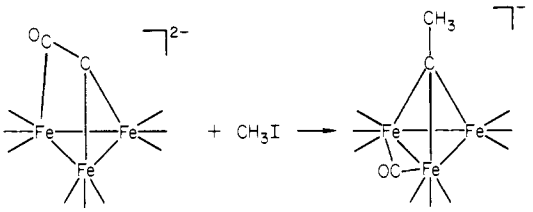

(5)

compound has recently been synthesized by a different method, and the spectroscopic parameters are in reasonable agreement.[22] They are also similar to those of the isoelectronic $H_3Fe_3(CO)_9(CCH_3)$.[23] In VII the ethylidyne resonance is observed at 289 ppm in the ^{13}C NMR, which is typical for this type of compound. The nature of this compound is further confirmed by the ^{13}C NMR, which shows no other resonances in the low-field region, thus precluding alkylation of the oxygen or carbon of the ketenylidyne CO.

Bonding. One straightforward way of viewing the bonding is to consider the ketenylidene dianion as a capping ligand to the $Fe_3(CO)_9$ cluster. The fragment treatment of similar systems by Hoffman and Schilling[24] shows that the 42 cluster valence electron $Fe_3(CO)_9$ (derived from the $Ru_3(CO)_{12}$-type structure by removal of axial ligands from one face) has three low-lying unfilled orbitals of a_1 and e symmetry. Correspondingly, the linear $[CCO]^{2-}$ moiety has three high-lying filled orbitals of a_1 and e symmetry that are favorably disposed for overlap with the $Fe_3(CO)_9$ orbitals (Figure 5). Thus the ligand can be viewed as a six-electron donor which will complete the 48 cluster valence electron count appropriate for a triangular cluster. This model explains the upright ketenylidene in $(\mu\text{-}H)_2Os_3(CO)_9(\mu_3\text{-}CCO)$ but does not reveal the origin of the tilt observed for CCO in $[Fe_3(CO)_9(CCO)]^{2-}$ (III).

Carbon suboxide (O=C=C=C=O) is a useful analogue of the ketenylidene because the linear molecule can be viewed as an adduct between CCO and CO, both of which have a_1 and e orbitals. The carbon suboxide molecule has bond lengths similar to those in III.[25] A symmetric infrared bending mode is observed

(22) Lourdichi, M.; Mathieu, R. *Nouv. J. Chim.* **1982**, *6*, 231.
(23) Wong, K. S.; Fehlner, T. P. *J. Am. Chem. Soc.* **1981**, *103*, 966.
(24) Schilling, B. E. R.; Hoffman, R. *J. Am. Chem. Soc.* **1979**, *101*, 3456.
(25) Livingston, R. L.; Rao, C. N. R. *J. Am. Chem. Soc.* **1959**, *81*, 285.

at very low frequency, and several calculations demonstrate that the π-system offers very little resistance to bending about the central carbon.[26] Similarly, there may be very little resistance to the tilt of the ketenylidene ligand in III. If the ketenylidene is as highly compliant as carbon suboxide, the tilt of the CCO ligand may arise from very weak interactions, such as weak nonbonded interactions or possibly a weak bonding interaction between the β-carbon of CCO and Fe2.

Another interpretation of the structure of III can be derived from ideas proposed by Bradley[27] for the four-iron butterfly system using Wade's rules.[28] Following this alternative approach, the C atom is considered to be part of the cluster rather than a ligand, and the cluster framework is therefore a pseudotetrahedron consisting of three iron atoms and one carbon atom. The CO coordinated to the carbide appears to be slightly semibridging across any iron–carbon bond. The iron carbonyl distance is within the postulated range of a semibridging CO.[5] This CO is then poised for migration onto the iron framework.

Acknowledgment. The research was supported by NSF Grant CHE-8204401. We appreciate an informative discussion with Dr. Kenneth Wade.

Registry No. II, 87710-96-1; III, 87698-63-3; IV, 83220-20-6; V, 87698-65-5; VI, 87698-64-4; VII, 87698-67-7; [PPN][$Fe_3(CO)_{10}(COCOCH_3)$], 69421-15-4.

Supplementary Material Available: Tables of anisotropic thermal parameters and observed and calculated structure factors for both molecules as well as bond distances and angles of the tetraphenylarsonium counterions of III (132 pages). Ordering information is given on any current masthead page.

(26) (a) Sabin, J. R.; Kim, H. *J. Chem. Phys.* **1972**, *56*, 2195. (b) Smith, W. H.; Leroi, G. E. *Ibid.* **1966**, *45*, 1784. (c) Olsen, J. F.; Burnelle, L. *J. Phys. Chem.* **1969**, *73*, 2298.

(27) Bradley, J. S.; Ansell, G. B.; Leonowicz, M. E.; Hill, E. W. *J. Am. Chem. Soc.* **1981**, *103*, 4968.

(28) Wade, K. *Adv. Inorg. Chem. Radiochem.* **1976**, *18*, 1.

Cation–Anion Combination Reactions. 24. Ionization Potentials, Solvation Energies, and Reactivities of Nucleophiles in Water[1]

Calvin D. Ritchie

Contribution from the Department of Chemistry, State University of New York at Buffalo, Buffalo, New York 14214. *Received June 2, 1983*

Abstract: An assumption is made and justified that free energies of bond dissociation in aqueous solution are approximately equal to enthalpies of bond dissociation in the gas phase. The free energies of bond dissociation in solution, thus estimated, are used in a thermochemical cycle to obtain free energies for one-electron transfer from various nucleophiles to the proton, standard electrode potentials vs. NHE for one-electron oxidations of the nucleophiles, and free energies of solution of the nucleophiles, all in aqueous solution. The one-electron oxidation potentials are shown to be correlated with the barriers to reactions of the nucleophiles with Pyronin cation [3,6-bis(dimethylamino)xanthylium cation]. The general problem of nucleophilic reactivity is discussed.

The experimental study of electrophile–nucleophile combination reactions has provided a wealth of data for testing various theories of nucleophilic reactivity.[1] It is fair to state that no general theory exists that is capable of giving even semiquantitative accord with the data.

One of the problems in attempts to formulate theories of nucleophilic reactivity is the sparsity of information on fundamental properties of the nucleophiles in solution. The only well-defined property for which data exist for a reasonable range of nucleophiles is basicity toward the proton, given by the pK_a's of the conjugate acids of the nucleophiles. Polarizabilities,[2] orbital energies,[3-5] hardness/softness,[6] and solvation energies[7] are some of the properties that have been postulated to affect reactivity but that are either poorly defined (hardness/softness), not presently obtainable for solution (anisotropic polarizability and orbital energies), or not generally available for species of interest (solvation energies).

For a few nucleophiles, the standard electrode potentials for oxidative dimerization

$$X^- = {}^1/_2X_2 + e^- \qquad (1)$$

are known and were once believed to be related to nucleophilic reactivity.[8] It was realized, however, that the bond dissociation energies of the X_2 species, which are an important variable component of the potentials for various X, should not be generally related to nucleophilic reactivity.[9] The relationship was modified[2] and later abandoned.[6]

The purpose of the present paper is to show that the standard electrode potentials for the half-cells

$$X^- = X\cdot + e^-$$
$$B = B^{+}\cdot + e^- \qquad (2)$$

for anionic, X^-, and neutral, B, nucleophiles can be estimated by

(1) A preliminary report of this work was presented at the 2nd Conference on Physical-Organic Chemistry, Florianopolis, Santa Catarina, Brazil, April 5–8 1983. For previous paper in this series, see: Ritchie, C. D. *J. Am. Chem. Soc.* **1983**, *105*, 3573.

(2) (a) Edwards, J. O. *J. Am. Chem. Soc.* **1956**, *78*, 1819. (b) Edwards, J. O.; Pearson, R. G. *J. Am. Chem. Soc.* **1962**, *84*, 16.

(3) Shaik, S. S.; Pross, A. *J. Am. Chem. Soc.* **1982**, *104*, 2708, and earlier references cited therein.

(4) Hudson, R. F. In "Chemical Reactivity and Reaction Paths"; Klopman, G., Ed.; Wiley-Interscience: New York, 1974; Chapter 5.

(5) Kolpman, G. In "Chemical Reactivity and Reaction Paths"; Klopman, G., Ed.; Wiley-Interscience: New York, 1974; Chapters 1 and 4.

(6) Pearson, R. G.; Songstad, J. *J. Am. Chem. Soc.* **1967**, *89*, 1827; Pearson, R. G. *J. Chem. Educ.* **1968**, *45*, 581, 643.

(7) Ritchie, C. D. *Acc. Chem. Res.* **1972**, *5*, 348.

(8) Edwards, J. O. *J. Am. Chem. Soc.* **1954**, *76*, 1540. For later development, see: Davis, R. E.; Nehring, R.; Blume, W. J.; Chuang, C. R. *J. Am. Chem. Soc.* **1969**, *91*, 91. Davis, R. E.; Suba, L.; Klimishin, P.; Carter, J. *J. Am. Chem. Soc.* **1969**, *91*, 104.

(9) Hawthorne, M. F.; Hammond, G. S.; Graybill, B. M. *J. Am. Chem. Soc.* **1955**, *77*, 486.

0002-7863/83/1505-7313$01.50/0